DOCMIA: DOCUMENT-LEVEL MEMBERSHIP INFERENCE ATTACKS AGAINST DOCVQA MODELS

Anonymous authors
Paper under double-blind review

ABSTRACT

Document Visual Question Answering (DocVQA) has introduced a new paradigm for end-to-end document understanding, and quickly became one of the standard benchmarks for multimodal LLMs. Automating document processing workflows, driven by DocVQA models, presents significant potential for many business sectors. However, documents tend to contain highly sensitive information, raising concerns about privacy risks associated with training such DocVQA models. One significant privacy vulnerability, exploited by the membership inference attack, is the possibility for an adversary to determine if a particular record was part of the model's training data. In this paper, we introduce two novel membership inference attacks tailored specifically to DocVQA models. These attacks are designed for two different adversarial scenarios: a white-box setting, where the attacker has full access to the model architecture and parameters, and a black-box setting, where only the model's outputs are available. Notably, our attacks assume the adversary lacks access to auxiliary datasets, which is more realistic in practice but also more challenging. Our unsupervised methods outperform existing state-of-the-art membership inference attacks across a variety of DocVQA models and datasets, demonstrating their effectiveness and highlighting the privacy risks in this domain.

1 INTRODUCTION

Automated document processing fuels a significant number of operations daily, ranging from fintech and insurance procedures to interactions with public administration and personal record keeping. Up until a few years ago, document processing services relied on template-based information extraction models, which were created ad-hoc for each client. Although these approaches allowed for good control of client data and could be extended to new documents with a few examples, they were limited in scalability and difficult to maintain. Consequently, the introduction of Document Visual Question Answering (DocVQA) Mathew et al. (2021) in 2019 has resulted in a paradigm shift in document processing services, enabling end-to-end generic solutions to be applied in this domain. DocVQA leverages multimodal large language models (LLMs) to streamline business workflows and provide clients with novel ways to interact with the document processing pipeline.

However, as cloud-based DocVQA solutions become more prevalent, significant privacy risks emerge, particularly concerning the potential leakage of sensitive information through model vulnerabilities. Indeed, during the training of a DocVQA model, each document can have several associated question-answer pairs, with each pair considered a unique training data point. As a result, a single document can appear multiple times in the dataset, which significantly raises the risks associated with privacy vulnerabilities. This repeated exposure enhances the likelihood of the model memorizing specific details, thereby increasing the potential for data leakage during privacy attacks. Furthermore, scanned document images often have high resolutions necessary for posterior analysis, but they need to be rescaled for processing by image encoders, potentially rendering content unreadable. To mitigate this issue, many DocVQA models utilize a dual representation of the document Huang et al. (2022); Tang et al. (2023), comprising both a reduced-scale image and OCR-recognized textual content. This approach introduces additional challenges, as sensitive information may leak through multiple modalities.

Membership inference attacks are among the most prominent techniques for assessing privacy vulnerabilities in machine learning models. These attacks enable an adversary to determine whether a

specific data point is included in the training dataset. However, there is limited research on membership inference risks in the context of multimodal models. Among the few studies, Ko et al. (2023); Hu et al. (2022) utilize powerful pre-trained models on large datasets to construct an aligned embedding space for the two modalities—image as input and text as output—allowing for the inference of membership information. Unfortunately, the reliance on these pre-trained models poses challenges for document-based tasks, particularly in DocVQA scenarios, where an alignment model capable of aligning the (document,question) as input and the answer as output is currently unavailable. Recently, Tito et al. (2024) introduced a provider-level membership inference attack against DocVQA models aimed at determining whether a provider (group) that may supply multiple invoice documents is part of the training dataset. In contrast, our research focuses on membership information at a finer granularity, specifically targeting the inference of whether a single document is included in the training dataset. Current MIA solutions that exploit standard features such as output logits, probabilities, or loss are difficult to adapt to the DocVQA context, where outputs are generated in an auto-regressive manner. Additionally, legal constraints surrounding copyright and private information complicate centralized model training, making it challenging to create auxiliary datasets that capture the variability and richness of real-world data. As a result, shadow training of proxy models becomes infeasible.

In this work, we take a structured approach to privacy testing for DocVQA models. We design a novel Document-level Membership Inference Attack (DocMIA), that deals with the multiple appearance of the same document in the training set. To overcome the difficulty in extracting typical metrics (e.g. logit-based) in this scenario of auto-regressive output generation, we propose a new method based on model optimisation for individual samples that allows us to generate novel, discriminative features for the DocMIA. We apply this approach to three different multimodal models. We propose attacks both for white-box and black-box models - to overcome the lack of auxiliary datasets we propose an alternative way for transfering knowledge from the attacked model to a proxy. We demonstrate that our methods yield state of the art results against a number of baseline methods.

To summarize, we make the following contributions:

1. We present the first document-level membership inference attacks specifically targeting multi-modal models for Document Visual Question Answering.
2. We introduce two novel auxiliary data-free attacks for both white-box and black-box settings, leveraging novel discriminative metrics for DocMIA.
3. We explore three distinct approaches to quantify these metrics: fine-tuning layers (FL), FLLoRA, and input gradients (IG).
4. Our attacks, evaluated on two benchmark datasets across three different models, outperform existing state-of-the-art membership inference attacks as well as baseline attacks.

2 Related Work

Membership Inference Attack. Membership inference attacks have been extensively explored in various applications to highlight privacy vulnerabilities in deep neural networks or to audit model privacy (Shokri et al., 2017). These attacks are categorized into two types: white-box and black-box settings. In white-box settings, the adversary has full access to the target model's internal parameters and computations (Carlini et al., 2022; Yeom et al., 2018; Nasr et al., 2019; Rezaei & Liu, 2021; Sablayrolles et al., 2019; Li & Zhang, 2021), enabling the use of informative features like loss values, logits, and gradient norms. Conversely, in black-box settings, the adversary is limited to the model's outputs, such as predicted labels or confidence scores (Choquette-Choo et al., 2021; Shokri et al., 2017; Salem et al., 2018; Sablayrolles et al., 2019; Song & Mittal, 2021; Hui et al., 2021). The literature indicates that white-box attacks tend to be more effective due to the availability of richer features (Song et al., 2019; Nasr et al., 2019). In this paper, we propose tailored attacks for both settings, considering a more challenging scenario where the adversary lacks an auxiliary dataset –which is used to train shadow models that mimic the behavior of the target model and are subsequently exploited to enhance attack performance– and is restricted to a limited number of queries. Regarding gradient-based membership inference attacks, research on using gradients as features has been limited. Nasr et al. (2019) leveraged the $L2$-norm of gradients with respect to model weights

for membership inference. Rezaei & Liu (2021) suggested using the distance to the decision boundary as a metric but found it ineffective for this purpose. In contrast, we introduce novel strategies called FL, FLLoRA, and IG, demonstrating that the $L2$-norm of the cumulative gradient—computed using these methods—provides a robust signal for membership inference. While Maini et al. (2021) and Li & Zhang (2021) also explored distance metrics, but from input points for membership inference in image classification tasks, their approaches lack scalability and applicability in our context, which involves larger-scale models with a wider vocabulary of tokens.

Membership Inference Attack Against Multi-modal Models. Research works into the privacy vulnerabilities of multi-modal models is still in its early stages. Recently, Tito et al. (2024); Pinto et al. (2024) proposed reconstruction attacks that exploit Document Visual Question Answering (DocVQA) model memorization to recover hidden values in documents. They black out specific target values in documents and query the model with questions about the modified documents. Since the model memorizes training data, it often reconstructs the hidden target values. Tito et al. (2024) also introduced a membership attack against DocVQA models to infer whether a document provider, with multiple documents, is included in the training dataset. However, as far as we know, no research has yet explored membership inference attacks at document-level granularity. Additionally, Ko et al. (2023); Hu et al. (2022) leverage powerful *pre-trained models* on large datasets to create an aligned embedding space for the two modalities to infer membership information. Unfortunately, the reliance on these pre-trained models introduces difficulties for document-based tasks, especially in Document Visual Question Answering (DocVQA) contexts, where an appropriate alignment model for aligning (document, question) inputs to corresponding answers is not yet available. Furthermore, the success of both attacks hinges on the availability of auxiliary datasets leveraged by the adversary, which are key to executing the attack effectively. In this paper, we present two membership inference attacks specifically tailored to tackle the unique characteristics of DocVQA models.

3 Background

3.1 Document-based Visual Question Answering

DocVQA is a multimodal task where natural language questions are posed based on the content of document images. Notably, it establishes a unified query-response framework applicable across various document understanding tasks, such as document classification, information extraction.

Formally, the DocVQA task is defined as follows: given a question-answer pair (q, a) related to a document image x, the method $\mathcal{F}$ must generate an answer $\hat{a} = \mathcal{F}(x, q)$ such that $\hat{a}$ closely matches the correct answer a. More concretely, given $D_t = \{(x_i, q_i, a_i)\}_{i=1}^{N_t}$ as a set of valid training examples, a model $\mathcal{F}$, parameterized by θ, is trained to maximize the conditional log-likelihood of the ground truth via the following loss:

$$\mathcal{L}(\theta) = -\log p_\theta(a_i|x_i, q_i) \tag{1}$$

Standard metrics for evaluating DocVQA include Accuracy (ACC) and Normalized Levenshtein Similarity (NLS) Biten et al. (2019), which measure the similarity between the predicted and correct answer. In the following sections, for clarity, we often omit the data example index i from the notation, unless referencing specific examples is essential for the discussion.

3.2 Document-level Membership Inference Attack

Membership Inference Attacks (MIAs) (Shokri et al., 2017) exploit privacy vulnerabilities to determine if a specific data point was included in the training set of a machine learning model. We extend this definition to the Document-level MIA, which is particularly suited in the DocVQA context.

Given access to a trained DocVQA model $\mathcal{F}$ and a document x drawn from its data distribution $\mathcal{D}$, along with a set of question-answer pairs $Q = \{(q_i, a_i)\}_{i=1}^{M}$ related to the information in the document, an adversary $\mathcal{A}$ designs a decision rule $f_{\mathcal{A}}(x, Q; \mathcal{F})$ to classify the membership status of x, aiming for $f_{\mathcal{A}}(x, Q; \mathcal{F}) = 1$ if x is a member of the training set, otherwise a non-member. It is important to note that the adversary is focused solely on *the membership of the document* x, rather than the entire DocVQA *data point* (x, q, a), which is typically the target of prior MI

attacks. Moreover, since a single document is associated with many question-answer pairs, this allows the adversary to query the same document using multiple questions that seek various pieces of information.

4 DocMIA against DocVQA models

In this section, we elaborate on the threat models relevant to the Document-level membership inference attacks we perform, focusing specifically on two scenarios: white-box and black-box access. We first explain our intuition behind our optimization-based attacks in the white-box setting, then adapt this approach to our black-box attacks.

4.1 Threat Model

MI attacks can be either a useful or harmful tool in various real-world scenarios, particularly when sensitive data such as documents are used to train ML models. On the positive side, MI attacks can act as a privacy auditing tool. For instance, in legal document processing, law firms may use MI attacks to evaluate whether proprietary or confidential documents, such as contracts or court filings, were included in model training, thereby identifying potential privacy risks. Conversely, MI attacks can be maliciously leveraged. As an example, a business competitor could exploit these attacks on an invoice-processing system to infer the presence of specific invoices in the training data, exposing confidential business relationships and leading to risks such as supplier poaching.

In both scenarios, we assume that the adversary aims to infer membership information for a test set of documents, determining whether each document is included in the training dataset. These documents may or may not be part of the target model's training data. Crucially, we further assume *the adversary lacks access to an auxiliary data* D_{aux} that reflects the characteristics of these test documents. This assumption is realistic, as obtaining real-world documents at scale is often prohibitively difficult due to their confidential nature and regulatory restrictions. Consequently, this negates the application of MI attack techniques that require training shadow models. Even if auxiliary documents were available, training numerous shadow document-based models—typically designed with a large number of parameters—would be prohibitively expensive.

Based on the previous examples, we refer to the owner of the document model as *the trainer* and the law firms or competitors as *the adversary*. Given the document distribution $\mathcal{D}$, the trainer trains a document-based model $\mathcal{F}_t$ with private access to $D_t \sim \mathcal{D}$, following a training algorithm $\mathcal{T}$, that defines the model architecture, optimization process, and related details. The adversary owns the set of sensitive documents $D_{\text{test}} \sim \mathcal{D}$, where $D_t \cap D_{\text{test}} \neq \emptyset$, $|D_{\text{test}}| = N_{\text{test}}$; but does not know which documents are in D_t. Given a document $x \in D_{\text{test}}$ with a set of related queries $Q = \{(q_i, a_i)\}_{i=1}^{M}$, the adversary's goal is to determine whether $x \in D_t$ or $x \notin D_t$.

We formulate two attack settings, which specify the adversarial knowledge about the model $\mathcal{F}_t$ and its data distribution $\mathcal{D}$:

White-box Setting. In this scenario, the adversary has full access to the internal workings of the target model, including the model's architecture, weights, gradients from any further training and other internal details. However, the adversary does not have access to the training algorithm $\mathcal{T}$.

Black-box Setting. Here, the adversary can only interact with the target model through an API, which only returns a prediction $\hat{a}$ for each question q on x. In addition, the adversary is constrained by a limited number of queries. As in the white-box setting, the adversary has no information about $\mathcal{T}$. This setting reflects the most challenging case (Nasr et al., 2019; Song et al., 2019). Additionally, we assume that the adversary possesses full knowledge of the DocVQA task for which the target model has been trained, including the common training objective and the types of documentsand the exact training questions. This assumption about the training objective/types of documents is realistic, as general task details are often available to provide users with instructions and guidelines, making such information accessible to adversaries as well. Assuming the knowledge of the exact questions is also plausible, as *an adversary can approximate them based on the knowledge of the training document type*. We discuss this assumption further and also conduct experiments in the setting without assuming the knowledge of exact training questions in the Appendix G.2.

4.2 WHITE-BOX DOCMIA

In the white-box setting, the adversary has access to the resulting model trained on private data. However, shadow training is not feasible, due to the unavailability of auxiliary dataset and the prohibitive cost of training if any, effectively ruling out the use of a supervised attack classifier. To this end, our strategy is to develop unsupervised *metric-based* attacks. Specifically, for each document in the attack test set, we optimize over the model parameters using one question-answer pair from that document. During this optimization, we extract a set of features that serve as signals for the membership inference attack. By repeating this process across all question-answer pairs for the document, we aggregate the features into a feature vector. Using these feature vectors, we apply an unsupervised clustering algorithm to separate member documents from non-members in the feature space. A critical component of our strategy is the selection of features that provide a discriminative descriptor for the clustering algorithm, enabling it to differentiate between the two membership classes. Some widely-studied metrics, such as logit and loss, may be challenging (as shown in Section 6) in this setting. Therefore, we opt to design new features, accompanied by a utility score, to form an informative feature vector for our attacks.

4.2.1 OPTIMIZATION-BASED DISCRIMINATIVE FEATURES

In this section, we introduce two novel discriminative membership features derived from an optimization process for our attacks against DocVQA models.

Intuition. Since DocVQA models are typically trained on multiple question-answer pairs per document, the model parameters likely converge to minimize the average distance to these ground-truth answers after training. As a result, fine-tuning the model on one question-answer pair through an iterative process is necessary to extract more reliable membership signals. More importantly, this optimization on training documents may converge faster than to non-training documents, due to the lower generalization error. Figure 1 illustrates our reasoning.

We provide a formal definition of the *distance* feature.

Definition 4.1 (Optimization-based Distance Feature). Given a model $\mathcal{F}$ parameterized by θ, let the model be initialized with θ_0. After undergoing a gradient-based optimization process $\mathcal{O}$, the parameters converge to θ^* according to a specified training objective $\mathcal{L}$. The *distance* feature is then defined as the $L2$-norm of the change in parameters:

$$\Delta(\theta_0, \theta^*) = ||\theta_0 - \theta^*||_2 \tag{2}$$

This feature measures the difference between the initial parameters θ_0 and the converged parameters θ^*, as an approximation of the optimization trajectory toward the optimal solution.

Specifically, we fine-tune the target DocVQA model on an individual document/question-answer pair and compute the *distance* required to reach the *optimal* answer. A small average distance indicates the document is likely part of the training set, while a larger distance suggests a non-training document. In addition, the number of optimization steps serves as an orthogonal feature that reflects the efficiency of the optimization process. With an optimal learning rate and a good initialization provided from the target model, optimization for training documents typically converges in fewer steps compared to non-training documents. Consequently, we include both the distance feature and the number of optimization steps in our feature set for white-box attacks.

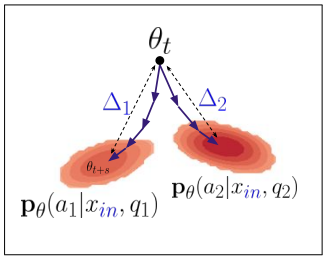

x^* is **in** of the training set

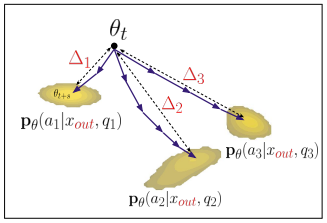

x^* is **out** of the training set

Figure 1: **Visualization of our fine-tuning strategy** in the parameters space. Each contour plot represents the optimization landscape with respect to each pair (a_i^*, q_i^*) from document x^*. In general, the average Δ computed by fine-tuning on member document $x^*_{\textbf{in}}$ is smaller than fine-tuning on non-member document $x^*_{\textbf{out}}$.

4.2.2 METHODOLOGY

We now formally present our attack strategy, assuming white-box access to the target model $\mathcal{F}_t$.

For any document $x \in D_{\text{test}}$ and a set of question-answer pairs Q, the goal is to assign a features descriptor F_x. This is achieved by first extracting a set of features through the optimization process $\mathcal{O}$ on a single question-answer pair. These features are aggregated across multiple questions then concatenated to construct F_x. Repeating this process over D_{test}, we apply an unsupervised clustering algorithm to differentiate member documents from non-members based on their features descriptors.

Following our intuition, for each question-answer pair (q, a), we fine-tune the target model parameter θ_t using gradient descent to maximize the conditional probability $p_\theta(a|x, q)$, as defined by the objective in Equation 1. The optimization process always starts from the target model parameters θ_t, and the learning rate α controls the optimization speed. During this process, we query the model at each step s using q, tracking its prediction quality against (q, a) via a utility function $\mathcal{U}$, either ACC or NLS. The optimization stops when no further improvements is observed, governed by a threshold τ or after a maximum of S steps. At the end of the optimization, we evaluate the distance Δ based on Equation 2, record the number of steps taken s, and aggregate the utility evolution throughout the process to obtain an overall DocVQA score u. Collectively, these features serve as membership signals for the current (q, a) pair in relation to the target document x.

Since each document is associated with a varying number of question-answer pairs M, we employ an aggregation function Φ to aggregate the features across all M questions, producing in a scalar value for each feature. Optionally, we can utilize a diverse set of aggregation functions to further enrich the feature set. After aggregation, we normalize all aggregated features to ensure they are on a consistent scale. The features descriptor F_x assigned to document x is constructed by concatenating these normalized features. The specific assignment algorithm for each document x is detailed in Algorithm 1 in the Appendix. Finally, we apply a clustering algorithm to the set of descriptors extracted from the target documents in D_{test} to differentiate members from non-members. We predict the cluster with the larger Δ to correspond to non-member documents.

Fine-tuning $\mathcal{F}_t$, as described above, can help differentiate between members and non-members. However, as the optimization must be performed on a *single* document/question-answer pair at a time, this approach is relatively slow given the model's size and the complexity of the data preprocessing. To address this and improve the efficiency of the attack, we introduce three variants of the method, as illustrated in Appendix Figure 5:

Optimize One Layer (FL). Instead of optimizing all parameters, we hope that gradients with respect to a single layer's parameters can provide sufficient signal for membership classification. In this variant, we select one specific layer L to optimize while keeping the remaining parameters fixed. We ablate the choice of layer for this method in Appendix D. In addition, we consider a variant leveraging LoRA Hu et al. (2021), termed **FLLoRA**, where the LoRA parameters are initialized with Kaiming initialization He et al. (2015). From Algorithm 1, we replace θ to θ_L or the LoRA parameters of the layer L, denoted as $\text{LoRA}(\theta_L)$, respectively.

Optimize the Document Image (IG). By switching the perspective to the input space, this variant directly optimizes the pixel values of the document image x. The underlying intuition remains the same: training documents require less self-tuning allowing the model to converge faster to the correct answer than non-trainings. However, this assumes the target model allows differentiation of the document image through its architecture. Accordingly, we replace θ with x from Algorithm 1 while freezing the target model parameters θ.

These variants reduce computational costs while maintaining attack performance, providing more practical options when the size of D_{test} increases.

4.3 BLACK-BOX DOCMIA

In the black-box setting, the attack model's access is restricted to D_{test} and the predicted *labels*. To address these limitations, we propose a distillation-based attack strategy. The key idea is to transfer knowledge about the private data D_t from the black-box model $\mathcal{F}_t$ to a proxy model $\mathcal{F}_p$, parameterized by ω. With full control over the proxy model, the attacks we design for the white-box setting can be fully applied to this proxy model.

Specifically, the black-box model is first employed to generate labels for each question in D_{test}, creating a query dataset $D_{\text{query}} = \{(x_i, Q_i)\}_{i=1}^{N_{\text{test}}}$ where $Q_i = \{(q_j, \mathcal{F}_{\theta_t}(x_i, q_j))\}_{j=1}^{M}$. The proxy model $\mathcal{F}_p$ is then trained on this query dataset, with the objective to maximize the likelihood of the predicted answer $p_\omega(\mathcal{F}_{\theta_t}(x_i, q_j)|x_i, q_j)$. In essence, the goal is to replicate the label-prediction behavior of the black-box model. By doing so, we aim to transfer the label space structure from the black-box to the proxy model, with the expectation that the membership features embedded in the black-box model will also be transferred, thus making our attack assumptions under white-box setting valid. Figure 5(c) illustrates the scheme of our proposed attack.

Since our focus is on the document domain, we initialize $\mathcal{F}_p$ using a publicly available checkpoint ω_{pt}, pre-trained with self-supervised learning on unlabeled document dataset D_{pt}, which is *inaccessible* and assumed to be *disjoint* from the private dataset D_t. This initialization equips the proxy model with a certain level of document understanding while ensuring it has no prior knowledge of the private dataset. As a result, it enables the proxy $\mathcal{F}_p$ to better mimic the prediction behavior and internal dynamics of the black-box model $\mathcal{F}_t$ after fine-tuning.

It is important to note that, in this scenario, the adversary lacks information of the black-box training algorithm $\mathcal{T}$. This means there is no advantage in terms of model architecture or other training details when constructing the proxy model. As a result, the choice of the proxy model, optimizer, learning rate, etc., is independent of the target model. However, as we demonstrate empirically in later sections (Section 6.1), while there is a clear benefit when the proxy model shares the same architecture as the black-box model, our attack strategies remain effective even when using entirely different architectures. This suggests that the proposed approach is robust and can be applied without relying on specific model classes or requiring detailed knowledge of the black-box model.

5 Experimental Setup

5.1 Target Dataset and Model

Target Dataset. We study two established DocVQA datasets in the literature for our analysis: **DocVQA (DVQA)** Mathew et al. (2021) and **PFL-DocVQA (PFL)** Tito et al. (2024). Both datasets are designed for extractive DocVQA tasks, where the answer text is explicitly found within the document image. Each document in these datasets is accompanied by varying number of questions that target various aspects of understanding and reasoning.

Target Model. We consider three state-of-the-art models which are designed for document understanding tasks models: (1) **Visual T5 (VT5)** Tito et al. (2024) (250M parameters) follows the traditional design by utilizing Optical Character Recognition (OCR) to facilitate the reasoning process. It leverages the T5 model, which is pre-trained on the C4 corpus Raffel et al. (2020), along with a Vision Transformer backbone that has been pre-trained on document data. (2) **Donut** Kim et al. (2022) (201M parameters) is one of the first end-to-end DocVQA models capable of achieving competitive performance without relying on OCR. It is pre-trained on a large collection of private synthetic documents. (3) **Pix2Struct** Lee et al. (2023) is another OCR-free document model available in two version: Base (282M parameters) and Large (1.3B parameters). This model is pre-trained to perform semantic parsing on an 80M subset of the C4 corpus. We utilize publicly available checkpoints from Hugging Face[1] Wolf et al. (2020).

For the PFL-DocVQA dataset, we consider two targets: VT5, using the public checkpoint provided by the authors[2], and Donut, which we successfully trained to achieve strong performance following the training procedure from the authors. For the DocVQA dataset, we attack four targets: VT5, Donut, and Pix2Struct (both Base and Large), all of which have publicly available checkpoints. In the black-box setting, we use VT5 and Donut as proxy models. To train the proxy models on the query set D_{query}, we initialize them with their public *pre-trained* checkpoints—the same checkpoints used to fine-tune the target models on the respective target datasets, as outlined in their respective papers. For more details on the models and datasets, please refer to Appendix A and E.

[1] https://huggingface.co/models

[2] https://benchmarks.elsa-ai.eu/?ch=2

	Model	SCORE-TA		SCORE-UA		SCORE-UA$_{all}$		LOSS-TA		GRADIENT-UA		SCORELOSS-UA$_{all}$		Min-K%†		Min-K%++†	
		ACC	F1	ACC	F1	ACC	F1	ACC	F1	ACC	F1	ACC	F1	ACC	F1	ACC	F1
PFL	VT5	**62.33**	**64.13**	$61.00_{0.0}$	$68.80_{0.0}$	$60.67_{0.0}$	$60.67_{0.0}$	57.83	62.81	$60.67_{0.0}$	$60.67_{0.0}$	$60.67_{0.0}$	$60.67_{0.0}$	57.17	64.84	**61.33**	**72.16**
	Donut	**73.33**	**75.14**	$68.33_{0.0}$	$75.77_{0.0}$	$71.17_{0.67}$	$71.33_{3.32}$	**73.67**	**78.99**	$70.67_{0.0}$	$69.55_{0.0}$	$70.83_{0.0}$	$69.67_{0.0}$	36.5	32.09	50.5	60.35
DVQA	VT5	**75.67**	**75.75**	$72.17_{0.0}$	$76.18_{0.0}$	$75.17_{0.0}$	$75.13_{0.0}$	73.67	77.99	$71.17_{0.0}$	$67.54_{0.0}$	**$75.50_{0.0}$**	**$76.02_{0.0}$**	71.0	76.16	66.67	74.56
	Donut	79.67	79.53	$75.97_{0.07}$	$79.57_{0.07}$	**$80.50_{0.0}$**	**$81.10_{0.0}$**	51.83	53.46	$77.17_{0.0}$	$75.92_{0.0}$	**$80.50_{0.0}$**	**$81.10_{0.0}$**	47.0	48.38	53.33	59.89
	Pix2Struct-B	67.33	67.97	**$68.17_{0.0}$**	**$71.36_{0.0}$**	$69.13_{0.07}$	$67.67_{0.09}$	59.33	64.63	$66.0_{0.0}$	$68.32_{0.0}$	**$69.00_{0.0}$**	**$67.48_{0.0}$**	68.0	72.8	54.50	66.99

Table 1: **Results from Baseline Attacks.**. **Gray** color indicate attacks conducted in the black-box setting. † indicates methods requiring grey-box access. Results are reported based on five random seeds for KMEANS, if any. The methods with the best *average* performance across the two metrics are highlighted in **bold**.

5.2 IMPLEMENTATION

Since the optimization process involves several hyperparameters; thus, our strategy is to tune the set of hyperparameters such that our attacks remain effective against each target model under white-box settings, which we then utilize to mount attacks on black-box models.

Assuming the knowledge of training algorithm $\mathcal{T}$ is unavailable for either white-box or black-box settings, we use Adam Kingma (2014) as the optimizer OPT and fix this choice across all our attack experiments. We explore the impact of learning rate α, the selected layer L, and we carefully tune the values of threshold τ in the ablation study (Appendix D). Following this, we select the optimal set of hyperparameters for each model and apply these settings in all black-box experiments. For the aggregation Φ, we consider 4 aggregation functions $\{\text{AVG}; \text{MIN}; \text{MAX}; \text{MED}\}$ for each feature, denoted as Φ_{all}. Throughout our experiments, we employ KMEANS as the clustering algorithm.

5.3 EVALUATION METRIC

Using the official split of each target dataset, we sample 300 member documents from the training split and 300 non-member documents from the test split, resulting a total of $N_{\text{test}} = 600$ test documents. We report **Balanced Accuracy** and **F1 score** as this evaluation metrics for the attack's success in the balanced setting, as in prior works (Salem et al., 2018; Watson et al., 2022; Ye et al., 2022). In addition, we evaluate our attacks using True Positive Rate (TPR) at 1% and 3% False Positive Rate (FPR), following standard practices in recent MIA literature Carlini et al. (2022). For all unsupervised attacks, including baseline methods, the membership score for each document is computed as the Euclidean distance between its feature vector and the centroid of the member cluster obtained via KMEANS.

5.4 BASELINE

In the *black-box* setting, we evaluate three MI attacks as baselines, which only requires the predicted answer to determine membership: Score-Threshold Attack (SCORE-TA), Unsupervised Score-based Attack (SCORE-UA) (Tito et al., 2024), and Unsupervised Score-based Attack with Φ_{all} (SCORE-UA$_{\text{all}}$).

For the *grey-box* setting, we consider two additional baselines: Min-K%Shi et al. (2023) and Min-K%++ Zhang et al. (2024), which assumes access to token-level probabilities of the generated answers to compute the membership score of each document.

In the *white-box* setting, where loss or gradient information is accessible, we evaluate three further baselines: Loss-Threshold Attack (LOSS-TA) (Yeom et al., 2018), and Unsupervised Score+Loss Attack (SCORELOSS-UA$_{\text{all}}$).

For detailed descriptions of these methods, we refer readers to Appendix C.

6 EVALUATION

6.1 WHITE-BOX SETTING

Baseline Performance Evaluation. Table 1 (*white*) shows the performance of baseline attacks in the white/gray-box setting. LOSS-TA, akin to the thresholding loss attack in Yeom et al. (2018), performs poorly on complex DocVQA models, achieving under 60% accuracy for most targets. In contrast, SCORELOSS-UA$_{\text{all}}$, which combines DocVQA scores and loss-based features, achieves stronger results: 81% F1 on Donut, 75% on VT5, and 69% on Pix2Struct. However, it underperforms LOSS-TA on PFL-DocVQA, with a 3% drop in accuracy and 8% in F1, likely due to high

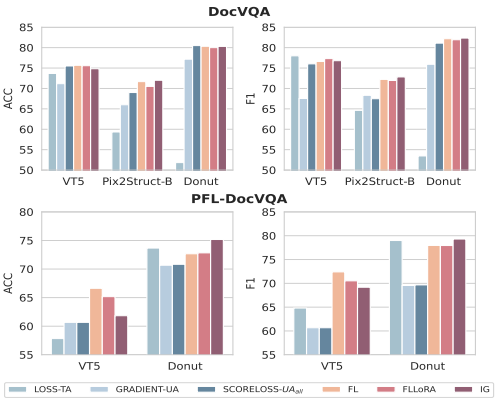

Figure 2: **White-box Setting: Our proposed attacks consistently achieve high performance**, generally outperforming the considered baselines.

	DVQA			PFL	
	VT5	Donut	Pix2Struct-B	VT5	Donut
LOSS-TA	**14.00**	7.67	5.33	3.00	**14.67**
GRADIENT-UA	9.33	6.00	5.00	3.00	8.33
SCORELOSS-UA$_{all}$	4.67	8.67	6.67	4.00	6.33
Min-K%	10.67	1.33	5.33	5.67	0.00
Min-K%++	7.00	9.33	10.33	8.00	2.00
FL	5.67	**10.67**	**11.00**	**8.67**	7.00
FLLoRA	11.33	5.33	6.33	3.33	10.00
IG	5.67	8.00	10.33	2.33	11.00

Table 2: **White-box Setting: TPR at 3% FPR**. Comparison across all white-box methods, with the best-performing method for each metric highlighted in **bold**. We refer the readers to Appendix F for the complete results.

loss variance in this dataset. GRADIENT-UA, , which incorporates one-step gradient information, matches the performance of score-based attacks, suggesting that the gradient serves as a useful signal for membership inference. None of the baseline methods generalizes well across all target models.

Our Proposed Attacks Outperform the Baselines. We evaluate our proposed attacks—FL, FLLoRA, and IG —in the white-box setting across target models. As shown in Figure 2, our methods consistently achieve high performance, indicating that *optimization-based features generalize well* across various models. Compared to all baselines, our attacks achieve either the best or near-best performance on both target datasets, with notable F1 scores of 72% against VT5 and Pix2Struct, and 82.5% against Donut. Against GRADIENT-UA, our optimization-based features yield up to a 10% improvement in F1 on Donut, indicating that *single-step gradients are insufficient* for reliable membership inference. From Table 2, our attacks consistently excel in the low-FPR regime, often surpassing or matching the strongest baselines. For instance, FL achieves a TPR of 8.67% at 3% FPR against VT5 (PFL-trained), despite minimal overfitting, and a TPR of 11.00% at the same FPR against Pix2Struct-B on DocVQA. Additionally, our methods outperform both Min-K% and Min-K%++ across all target models, underscoring their effectiveness, particularly for DocMIA setting. These results highlight the privacy risks posed by optimization-based features in membership inference. For full results and in-depth analysis, please refer to Appendices F and G.

Why Are Our Proposed Attacks More Effective? We evaluate the effectiveness of our optimization-based features compared to traditional metrics such as loss or single-gradient norms.

The Loss-based attack LOSS-TA assumes that member documents exhibit lower loss values than non-member documents after training the target model $\mathcal{F}_t$. While this approach leverages the generalization gap, it proves too simplistic for large-scale models that are trained with complex training process to minimize overfitting. The generalization capability of these models, especially in DocVQA tasks, often reduces the sensitivity of the loss as a membership indicator. Our attacks, on the other hand, leverage the optimization landscape with respect to the model parameters, *conditioned on each question-answer pair*. We hypothesize that the distance resulting from parameter optimization pairs from a member document will be smaller compared to those for a non-member document, as depicted in Figure 1. This fine-grained signal, which reflects the model's internal response to optimization, offers a more discriminative feature for identifying membership.

As illustrated in Appendix, Figure 8, our *distance* feature, derived from the optimization process, provides a better separation between members and non-members compared to loss-based methods (Figure 7 (*top*)). The t-SNE visualization van der Maaten & Hinton (2008) from Figure 7 (*bottom*) further demonstrates that features derived from our attacks yield a more distinct clustering of member and non-member documents in high-dimensional space for all target models, underscoring its efficacy as a membership indicator, therefore outperforms the loss-based approach.

6.2 BLACK-BOX SETTING

Baseline Performance Evaluation. Table 1 (*gray*) presents the results of our black-box baseline attacks, all of which rely on the DocVQA score as the only source of information in this setting.

	Proxy Model	VT5					
	Black-box	FL		FLLoRA		IG	
		ACC	F1	ACC	F1	ACC	F1
PFL	**VT5**	$63.33_{0.0}(+2.33)$	$69.51_{0.03}(+0.71)$	$63.33_{0.0}(+2.33)$	$69.01_{0.0}(+0.21)$	$62.00_{0.16}(+1)$	$69.35_{0.2}(+0.55)$
	Donut	$70.83_{0.0}(-0.34)$	$76.64_{0.0}(+0.87)$	$70.83_{0.0}(-0.34)$	$76.70_{0.0}(+0.93)$	$70.67_{0.0}(-0.5)$	$76.72_{0.0}(+0.95)$
DVQA	**VT5**	$74.33_{0.01}(-0.84)$	$75.08_{0.0}(-1.1)$	$74.33_{0.0}(-0.84)$	$74.67_{0.0}(-1.51)$	$73.83_{0.08}(-1.34)$	$75.81_{0.0}(-0.37)$
	Donut	$81.67_{0.0}(+1.17)$	$82.54_{0.0}(+1.44)$	$81.17_{0.0}(+0.67)$	$82.09_{0.0}(+0.99)$	$80.17_{0.0}(-0.33)$	$81.89_{0.0}(+0.79)$
	Pix2Struct-B	$70.17_{0.0}(+1.04)$	$69.71_{0.0}(-1.65)$	$70.27_{0.23}(+1.14)$	$70.85_{0.07}(-0.51)$	$71.17_{0.0}(+2.04)$	$72.14_{0.0}(+0.78)$
	Pix2Struct-L	$71.67_{0.01}(+0.84)$	$72.13_{0.0}(+1.30)$	$70.17_{0.0}(-0.66)$	$71.27_{0.0}(+0.44)$	$71.00_{0.05}(+0.17)$	$73.15_{0.0}(+2.32)$
	Proxy Model	Donut					
PFL	**VT5**	$61.73_{0.08}(+0.73)$	$64.04_{0.10}(-4.76)$	$61.67_{0.08}(+0.67)$	$63.49_{0.0}(-5.31)$	$55.17_{0.17}(-5.83)$	$57.37_{0.3}(-11.43)$
	Donut	$72.17_{0.0}(+2.33)$	$76.24_{0.0}(-0.19)$	$72.67_{0.0}(+1.5)$	$77.47_{0.0}(+1.7)$	$74.50_{0.0}(+3.33)$	$76.43_{0.0}(+0.66)$
DVQA	**VT5**	$73.50_{0.0}(-4.34)$	$75.58_{0.0}(-4.36)$	$74.17_{0.0}(-1)$	$76.04_{0.0}(-0.14)$	$74.0_{0.0}(-1.17)$	$75.93_{0.01}(-0.25)$
	Donut	$79.50_{0.0}(-1)$	$81.50_{0.0}(+0.4)$	$80.0_{0.0}(-0.5)$	$81.82_{0.0}(+0.72)$	$80.27_{0.0}(-0.23)$	$81.96_{0.0}(+0.86)$
	Pix2Struct-B	$70.83_{0.0}(+3.04)$	$71.82_{0.0}(+4.88)$	$70.83_{0.06}(+1.70)$	$71.73_{0.14}(+0.37)$	$71.0_{0.01}(+1.87)$	$71.94_{0.0}(+0.58)$
	Pix2Struct-L	$70.83_{0.0}(0)$	$72.95_{0.0}(+2.12)$	$71.0_{0.0}(+0.17)$	$72.98_{0.0}(+2.15)$	$71.0_{0.03}(+0.17)$	$72.81_{0.01}(+1.98)$

Table 3: **Black-Box Setting: Main Results of Black-Box DocMIA using Donut and VT5 as proxy models**. The checkpoints for the **black-box models** are trained on the respective datasets. Values in parentheses indicate the improvement (positive/negative) compared to the *best* number from SCORE-UA-based baselines. Results are reported over five random seeds.

	Target	DVQA				PFL	
		VT5	**Donut**	**P2S-B**	**P2S-L**	**VT5**	**Donut**
	SCORE-TA	9.33	11.00	9.00	**9.00**	5.00	2.67
	SCORE-UA	7.67	15.67	6.67	6.67	3.33	3.33
	$\text{SCORE-UA}_{\text{all}}$	9.33	11.00	9.00	9.00	5.00	2.67
VT5	FL	12.33	**23.00**	**16.67**	5.33	2.00	**8.00**
	FLLoRA	**11.33**	23.00	9.33	4.67	3.33	2.00
	IG	8.33	7.00	7.67	7.00	3.67	6.67
Donut	FL	6.33	4.00	4.67	7.33	1.33	4.00
	FLLoRA	6.33	4.00	6.33	8.00	5.33	5.33
	IG	5.00	11.00	9.33	6.33	**6.33**	4.33

Table 4: **Black-box Setting: TPR at 3% FPR using Donut and VT5 as proxy models**. Comparison across all black-box methods, with the best-performing method for each metric highlighted in **bold**. The complete results can be found in the Appendix F.

Similar to the loss metric, the score metric is directly correlated with the generalization gap, making attacks more effective when there is a higher degree of overfitting. This trend is illustrated in Figure 9, where we observe strong MI performance, particularly for the Donut model with 75% in PFL and 79% F1 score in DocVQA. Meanwhile, both SCORE-UA-based baselines show comparable performance, especially effective against models trained on DocVQA. Overall, no single method emerges as the clear winner across all target models.

Our Black-box Attacks outperforms the Baselines. Table 3 presents the key results of our proposed black-box attacks using two proxy models, VT5 and Donut. Several important observations can be made:

First, we observe a clear advantage of attacking the proxy models distilled with our proposed techniques. Across a wide range of black-box architectures trained on both target datasets, attacks leveraging the proxy models outperform the black-box baselines in most cases, demonstrating better MI performance. This suggests that, even without knowledge of the black-box model architecture, *one chosen proxy model still effectively distills certain behaviors* from the black-box models which are membership-indicative, enabling our attacks to infer membership with high accuracy.

When the architecture of the black-box model matches that of the proxy, we consistently observe improvements in MI performance. This is particularly evident on the PFL-DocVQA dataset when using both proxy models to attack *black-box models of the same type*.

Among the target, *Pix2Struct proves to be the most vulnerable* (both Base and Large versions). Both VT5 and Donut proxies gains of +3.04% in Accuracy and +4.88% in F1 score over the best baseline, even against the Pix2Struct-Large model, which exhibits strong generalization and a minimal Train-Test gap (Figure 9).

Overall, using VT5 as a proxy yields robust results, achieving TPRs of 23.00% and 16.67% against Donut and Pix2Struct-B, respectively, at 3% FPR on DocVQA, as shown in Table 4 . This aligns with the observed Train-Test utility gaps in target models (Table 10), allowing proxies to closely replicate black-box predictions and enhance attack success.

These results suggest that privacy vulnerabilities can be exploited under black-box settings, using simple distillation-based strategies applied to the model's output space.

7 CONCLUSION

In this paper, we introduce the first document-level membership inference attacks for Document Visual Question Answering (DocVQA) models, addressing privacy risks in multimodal contexts. By employing a structured approach that leverages model optimization techniques, we extract meaningful features that navigate the challenges posed by the intricacies of multimodal data, the frequent presence of documents in training datasets, and autoregressive outputs. This enables us to propose novel, auxiliary, data-free attack methods for both white-box and black-box scenarios. Our results, validated across multiple datasets and models, significantly outperform existing membership inference baselines, underscoring the critical privacy risks in DocVQA models and the urgent need for enhanced privacy measures in this rapidly evolving field.

8 Ethics Statement

Our research introduces two novel membership inference attacks on Document Visual Question Answering (DocVQA) models, designed to evaluate the privacy risks inherent in such systems. While our methodology exposes vulnerabilities that could potentially be exploited for malicious purposes, the primary objective of this work is to raise awareness about privacy issues in AI systems, specifically in the context of DocVQA models, and to encourage the development of more privacy-preserving technologies.

9 Reproducibility Statement

In this work, we have made several efforts to ensure the reproducibility of our results. We utilize public datasets and open-source models, which are clearly described in Section 5.1. The implementation details of our proposed membership inference attacks are thoroughly presented in Section 5.2 and Appendix E. Additionally, all relevant hyperparameters used in our experiments are provided in the appendix, offering detailed information for reproducing our results. We will provide a link to the code for the camera-ready version, enabling future researchers to replicate and extend our work with ease.

References

Martin Abadi, Andy Chu, Ian Goodfellow, H Brendan McMahan, Ilya Mironov, Kunal Talwar, and Li Zhang. Deep learning with differential privacy. In Proceedings of the 2016 ACM SIGSAC conference on computer and communications security, pp. 308–318, 2016.

Borja Balle, Gilles Barthe, Marco Gaboardi, Justin Hsu, and Tetsuya Sato. Hypothesis testing interpretations and renyi differential privacy. In International Conference on Artificial Intelligence and Statistics, pp. 2496–2506. PMLR, 2020.

Ali Furkan Biten, Ruben Tito, Andres Mafla, Lluis Gomez, Marçal Rusinol, Ernest Valveny, CV Jawahar, and Dimosthenis Karatzas. Scene text visual question answering. In Proceedings of the IEEE/CVF international conference on computer vision, pp. 4291–4301, 2019.

Nicholas Carlini, Steve Chien, Milad Nasr, Shuang Song, Andreas Terzis, and Florian Tramer. Membership inference attacks from first principles. In 2022 IEEE Symposium on Security and Privacy (SP), pp. 1897–1914. IEEE, 2022.

Christopher A Choquette-Choo, Florian Tramer, Nicholas Carlini, and Nicolas Papernot. Label-only membership inference attacks. In International conference on machine learning, pp. 1964–1974. PMLR, 2021.

Cynthia Dwork, Aaron Roth, et al. The algorithmic foundations of differential privacy. Foundations and Trends® in Theoretical Computer Science, 9(3–4):211–407, 2014.

Kaiming He, Xiangyu Zhang, Shaoqing Ren, and Jian Sun. Delving deep into rectifiers: Surpassing human-level performance on imagenet classification. In Proceedings of the IEEE international conference on computer vision, pp. 1026–1034, 2015.

Edward J Hu, Yelong Shen, Phillip Wallis, Zeyuan Allen-Zhu, Yuanzhi Li, Shean Wang, Lu Wang, and Weizhu Chen. Lora: Low-rank adaptation of large language models. arXiv preprint arXiv:2106.09685, 2021.

Pingyi Hu, Zihan Wang, Ruoxi Sun, Hu Wang, and Minhui Xue. M^4 i: Multi-modal models membership inference. Advances in Neural Information Processing Systems, 35:1867–1882, 2022.

Yupan Huang, Tengchao Lv, Lei Cui, Yutong Lu, and Furu Wei. Layoutlmv3: Pre-training for document ai with unified text and image masking. In Proceedings of the 30th ACM International Conference on Multimedia, pp. 4083–4091, 2022.

Bo Hui, Yuchen Yang, Haolin Yuan, Philippe Burlina, Neil Zhenqiang Gong, and Yinzhi Cao. Practical blind membership inference attack via differential comparisons. arXiv preprint arXiv:2101.01341, 2021.

Albert Q Jiang, Alexandre Sablayrolles, Arthur Mensch, Chris Bamford, Devendra Singh Chaplot, Diego de las Casas, Florian Bressand, Gianna Lengyel, Guillaume Lample, Lucile Saulnier, et al. Mistral 7b. arXiv preprint arXiv:2310.06825, 2023.

Geewook Kim, Teakgyu Hong, Moonbin Yim, JeongYeon Nam, Jinyoung Park, Jinyeong Yim, Wonseok Hwang, Sangdoo Yun, Dongyoon Han, and Seunghyun Park. Ocr-free document understanding transformer. In Shai Avidan, Gabriel Brostow, Moustapha Cissé, Giovanni Maria Farinella, and Tal Hassner (eds.), Computer Vision – ECCV 2022, pp. 498–517, Cham, 2022. Springer Nature Switzerland. ISBN 978-3-031-19815-1.

Diederik P Kingma. Adam: A method for stochastic optimization. arXiv preprint arXiv:1412.6980, 2014.

Myeongseob Ko, Ming Jin, Chenguang Wang, and Ruoxi Jia. Practical membership inference attacks against large-scale multi-modal models: A pilot study. In Proceedings of the IEEE/CVF International Conference on Computer Vision, pp. 4871–4881, 2023.

Kenton Lee, Mandar Joshi, Iulia Turc, Hexiang Hu, Fangyu Liu, Julian Eisenschlos, Urvashi Khandelwal, Peter Shaw, Ming-Wei Chang, and Kristina Toutanova. Pix2struct: screenshot parsing as pretraining for visual language understanding. In Proceedings of the 40th International Conference on Machine Learning, ICML'23. JMLR.org, 2023.

Zheng Li and Yang Zhang. Membership leakage in label-only exposures. In Proceedings of the 2021 ACM SIGSAC Conference on Computer and Communications Security, pp. 880–895, 2021.

Pratyush Maini, Mohammad Yaghini, and Nicolas Papernot. Dataset inference: Ownership resolution in machine learning. 2021.

Minesh Mathew, Dimosthenis Karatzas, and CV Jawahar. Docvqa: A dataset for vqa on document images. In Proceedings of the IEEE/CVF winter conference on applications of computer vision, pp. 2200–2209, 2021.

Milad Nasr, Reza Shokri, and Amir Houmansadr. Comprehensive privacy analysis of deep learning: Passive and active white-box inference attacks against centralized and federated learning. In 2019 IEEE symposium on security and privacy (SP), pp. 739–753. IEEE, 2019.

Francesco Pinto, Nathalie Rauschmayr, Florian Tramèr, Philip Torr, and Federico Tombari. Extracting training data from document-based VQA models. In Proceedings of the 41st International Conference on Machine Learning, Proceedings of Machine Learning Research, pp. 40813–40826. PMLR, 2024.

Colin Raffel, Noam Shazeer, Adam Roberts, Katherine Lee, Sharan Narang, Michael Matena, Yanqi Zhou, Wei Li, and Peter J Liu. Exploring the limits of transfer learning with a unified text-to-text transformer. Journal of machine learning research, 21(140):1–67, 2020.

Shahbaz Rezaei and Xin Liu. On the difficulty of membership inference attacks. In Proceedings of the IEEE/CVF Conference on Computer Vision and Pattern Recognition, pp. 7892–7900, 2021.

Alexandre Sablayrolles, Matthijs Douze, Cordelia Schmid, Yann Ollivier, and Herve Jegou. White-box vs black-box: Bayes optimal strategies for membership inference. In Proceedings of the 36th International Conference on Machine Learning, pp. 5558–5567. PMLR, 2019.

Ahmed Salem, Yang Zhang, Mathias Humbert, Pascal Berrang, Mario Fritz, and Michael Backes. Ml-leaks: Model and data independent membership inference attacks and defenses on machine learning models. arXiv preprint arXiv:1806.01246, 2018.

Weijia Shi, Anirudh Ajith, Mengzhou Xia, Yangsibo Huang, Daogao Liu, Terra Blevins, Danqi Chen, and Luke Zettlemoyer. Detecting pretraining data from large language models. arXiv preprint arXiv:2310.16789, 2023.

Reza Shokri, Marco Stronati, Congzheng Song, and Vitaly Shmatikov. Membership inference attacks against machine learning models. In 2017 IEEE symposium on security and privacy (SP), pp. 3–18. IEEE, 2017.

Liwei Song and Prateek Mittal. Systematic evaluation of privacy risks of machine learning models. In 30th USENIX Security Symposium (USENIX Security 21), pp. 2615–2632, 2021.

Liwei Song, Reza Shokri, and Prateek Mittal. Privacy risks of securing machine learning models against adversarial examples. In Proceedings of the 2019 ACM SIGSAC conference on computer and communications security, pp. 241–257, 2019.

Zineng Tang, Ziyi Yang, Guoxin Wang, Yuwei Fang, Yang Liu, Chenguang Zhu, Michael Zeng, Cha Zhang, and Mohit Bansal. Unifying vision, text, and layout for universal document processing. In Proceedings of the IEEE/CVF conference on computer vision and pattern recognition, pp. 19254–19264, 2023.

Rubèn Tito, Khanh Nguyen, Marlon Tobaben, Raouf Kerkouche, Mohamed Ali Souibgui, Kangsoo Jung, Joonas Jälkö, Vincent Poulain D'Andecy, Aurelie Joseph, Lei Kang, et al. Privacy-aware document visual question answering. In International Conference on Document Analysis and Recognition, pp. 199–218. Springer, 2024.

Laurens van der Maaten and Geoffrey Hinton. Visualizing data using t-sne. Journal of Machine Learning Research, pp. 2579–2605, 2008.

A Vaswani. Attention is all you need. Advances in Neural Information Processing Systems, 2017.

Lauren Watson, Chuan Guo, Graham Cormode, and Alexandre Sablayrolles. On the importance of difficulty calibration in membership inference attacks. In International Conference on Learning Representations, 2022.

Thomas Wolf, Lysandre Debut, Victor Sanh, Julien Chaumond, Clement Delangue, Anthony Moi, Pierric Cistac, Tim Rault, Remi Louf, Morgan Funtowicz, Joe Davison, Sam Shleifer, Patrick von Platen, Clara Ma, Yacine Jernite, Julien Plu, Canwen Xu, Teven Le Scao, Sylvain Gugger, Mariama Drame, Quentin Lhoest, and Alexander Rush. Transformers: State-of-the-art natural language processing. In Qun Liu and David Schlangen (eds.), Proceedings of the 2020 Conference on Empirical Methods in Natural Language Processing: System Demonstrations, pp. 38–45, Online, 2020. Association for Computational Linguistics.

Jiayuan Ye, Aadyaa Maddi, Sasi Kumar Murakonda, Vincent Bindschaedler, and Reza Shokri. Enhanced membership inference attacks against machine learning models. In Proceedings of the 2022 ACM SIGSAC Conference on Computer and Communications Security, pp. 3093–3106, 2022.

Samuel Yeom, Irene Giacomelli, Matt Fredrikson, and Somesh Jha. Privacy risk in machine learning: Analyzing the connection to overfitting. In 2018 IEEE 31st computer security foundations symposium (CSF), pp. 268–282. IEEE, 2018.

Jingyang Zhang, Jingwei Sun, Eric Yeats, Yang Ouyang, Martin Kuo, Jianyi Zhang, Hao Frank Yang, and Hai Li. Min-k%++: Improved baseline for detecting pre-training data from large language models. arXiv preprint arXiv:2404.02936, 2024.

TABLE OF CONTENTS

A DOCVQA DATASET

DocVQA Mathew et al. (2021) This dataset contains high-quality human annotations and is widely used as a benchmark for document understanding. It comprises of real-world administrative documents across a diverse range of types, including letters, invoices, and financial reports.

PFL-DocVQA Tito et al. (2024) A large-scale dataset of real business invoices, often containing privacy-sensitive information such as payment amounts, tax numbers, and bank account details. This dataset is specifically designed for DocVQA tasks in a federated learning and differential privacy setup, supporting different levels of privacy granularity. The dataset is accompanied by a variant of MI attacks, where the goal is to infer the membership of the invoice's owner (i.e., the provider) from a set of their invoices that were not used during training.

	DocVQA		PFL-DocVQA	
Split	Num. Docs	Num. Questions	Num. Docs	Num. Questions
Train	69894	221316	10194	39463
Val	9150	30491	1286	5349
Test	13463	43591	1287	5188

Table 5: **Statistics** from PFL and DocVQA dataset.

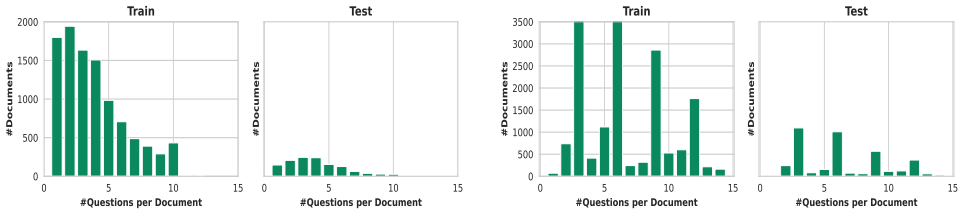

(a) **DocVQA** (b) **PFL-DocVQA**

Figure 3: Updated content: **The distribution of number per-document questions** from PFL and DocVQA dataset.

In Table 5, we present statistics for both the DocVQA and PFL-DocVQA datasets, focusing on their sizes. Additionally, Figure 3 illustrates the distribution of the number of questions per document. Notably, the distribution is relatively skewed: (1) while a small subset of documents have more than 10 questions, the majority contain fewer than 10 questions, and (2) a small fraction of documents are associated with a single question. These trends are consistent across both datasets.

B Document-level Membership Inference Attacks

We demonstrate the scheme of Document-level Membership Inference Attacks in Figure 4.

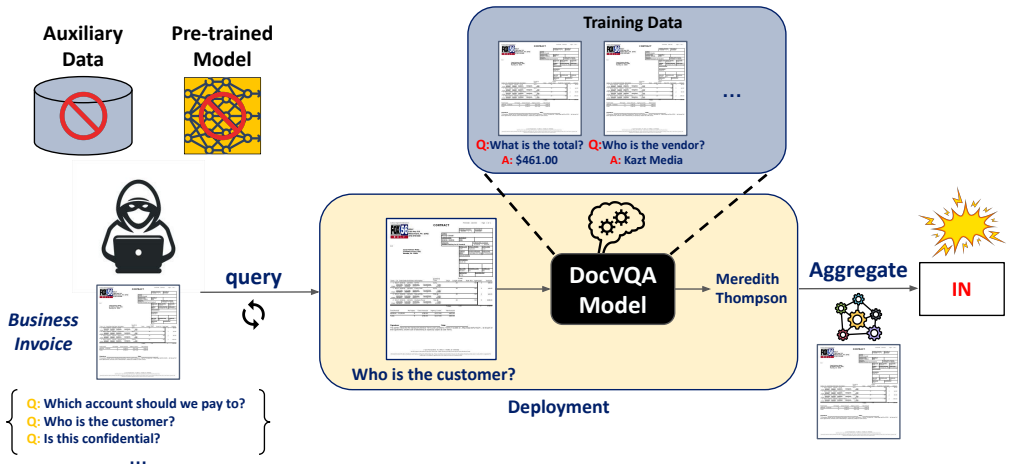

Figure 4: **The General Scheme of Document-level Membership Inference Attacks.** *Training:* A DocVQA model has been trained on a dataset comprising a set of documents, each associated with **multiple questions/answers**. *Inference/Deployment:* an adversary exploits this structure by querying the model with several questions related to a target document. By aggregating the model's response patterns, the adversary can infer the membership status of the document in the training set. This demonstrates a significant privacy vulnerability in document-based models.

Figure 5 illustrates the overall designs of our propose attacks, which revolves around leveraging optimization-based techniques to infer the membership status of a document. By systematically optimizing model parameters on individual question-answer pairs, DocMIA extracts discriminative features that reveal whether a document was part of the training set. Our method applies to both white-box and black-box models and integrates multiple features for a robust attack.

We also detail the steps of our proposed attack in the Algorithm 1, highlighting the key operations involved in feature extraction and membership prediction.

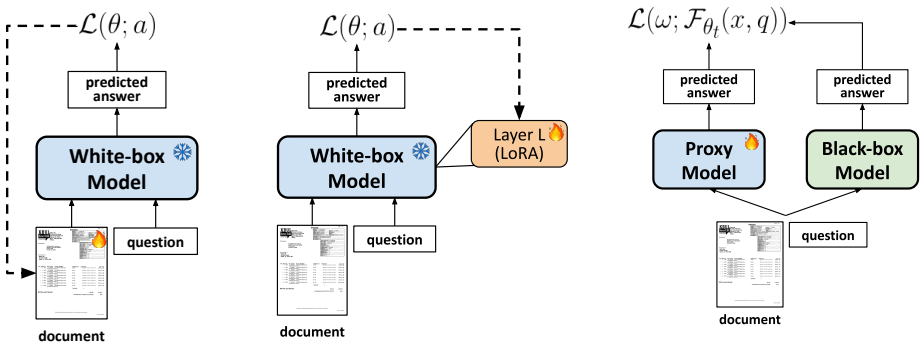

(a) Optimize the Document (b) Optimize One Layer (c) Distill the Black-box

Figure 5: **Variants of our proposed DocMIA.** Left: (a) (b) illustrate three attack strategies in the white-box setting: optimizing either the Document Image or a Single Layer (LoRA). Dashed arrows indicate the back-propagated gradient during optimization. Right: We distill the black-box into a proxy model, which is then attacked using the white-box strategies.

Algorithm 1 DocMIA Assignment

Input: target model $\mathcal{F}_{\theta_t}$, target document $x \in D_{\text{test}}$, question-answer pairs $\{(q_i, a_i)\}_{i=1}^{M}$, utility function $\mathcal{U}$, aggregation function Φ.
Hyperparameters: optimization steps S, optimizer OPT, learning rate α, threshold τ.
for $i = 1$ **to** M **do**
  Set θ.requires_grad = True // Change θ to: θ_L or LoRA(θ_L) or x and Freeze θ.
  Initialize: $s_i = 0, u_i = \{\}; l_i \leftarrow 0, \theta_0 \leftarrow \theta_t$
  while $s_i < S$ **do**
    $u_i \leftarrow u_i \cup \mathcal{U}(\mathcal{F}_\theta(x, q_i), a_i)$
    if $(\mathcal{L}(\theta) - l) < \tau$ **then** break; // Early stopping
    end if
    $\theta \leftarrow \text{OPT}(\alpha, \nabla_\theta(\mathcal{L}(\theta))$
    $l_i \leftarrow \mathcal{L}(\theta), s_i \leftarrow s_i + 1$
  end while
  $\Delta_i \leftarrow \|\theta_0 - \theta\|$ // Compute distance metric
end for
$\Delta_M = \Phi(\Delta_{i=1,\ldots,M}); s_M = \Phi(s_{i=1,\ldots,M}); u_M = \Phi(u_{i=1,\ldots,M})$ // Aggregating over M questions
Output: $F_x = [\Delta_M, s_M, u_M]$ // Assign membership feature vector

C Attack Baselines

For the *black-box* setting, we evaluate three MI attacks as baselines, which only requires generated text to infer the membership of the target document:

Score-Threshold Attack (Score-TA) assumes that training documents should achieve higher scores than non-training ones. This attack, adapted from Yeom et al. (2018), evaluates the prediction $\hat{a}$ for each question q using the utility function $\mathcal{U}$ and computes the average score $\bar{u}$. A document is then predicted as a member $\bar{u} \geq \kappa$, and non-member otherwise. The threshold κ is set as the average value of $\bar{u}$ across D_{test}.

Unsupervised Score-based Attack (Score-UA) Tito et al. (2024). This attack applies an unsupervised clustering algorithm over the set of average score $\bar{u}$ from test documents in D_{test}, documents within the cluster with higher average score are predicted as members.

Unsupervised Score-based Attack - An Extension (Score-UA$_{\text{all}}$). This attack extends Score-UA by considering multiple aggregation functions Φ_{all} to form the feature vector.

For the *grey-box* setting, we consider two additional baselines which assumes access to token-level probabilities of the generated answers a to compute the membership score of each document:

Min-K% Shi et al. (2023) computes the average log probability of the lowest-K% answer tokens as the membership score: Min-K% $= \frac{1}{|\text{Min-K\%}(a)|}\Sigma_{a_i \in \text{Min-K}(a)} \log p(a_i|a_{<i})$. Intuitively, training documents are less likely to contain low-probability answer tokens, resulting in higher scores.

Min-K%++ Zhang et al. (2024) also averages scores from the lowest-K% probability tokens but assumes that tokens in the predicted answers for training documents have high probabilities or often form the mode of the conditional distribution. Thus, for each token, the score is computed as: Min-K%++$(a_{<i}, a_i) = \frac{\log p(a_i|a_{<i}) - \mu_{a_{<t}}}{\sigma_{a_{<t}}}$ with $\mu_{a_{<t}}$ and $\sigma_{a_{<t}}$ are the expectation and standard deviation of $p(a_i|a_{<i})$ respectively.

We adapt these baselines to DocMIA by using an AVG aggregation function to combine scores across question-answer pairs within a document. We evaluated $K \in [0.6, 0.7, 0.8, 0.9, 1.0]$, which correspond to corresponds to 60% to 100% the length of the answer and reported the best result.

In the *white-box* setting, where loss information is available, we consider three additional baselines:

Loss-Threshold Attack (LOSS-TA) Yeom et al. (2018) Similar to SCORE-TA, this attack computes the average loss $\bar{l} = \frac{1}{M}\Sigma_i^M \mathcal{L}(\mathcal{F}(x, q_i))$. A document is predicted as a member if $\bar{l} \leq \kappa$ and otherwise non-member, where κ is selected as the average value of $\bar{l}$ across D_{test}.

Unsupervised One-step Gradient Attack (GRADIENT-UA) Inspired from Nasr et al. (2019), this attack utilizes the average norm of the gradient of the loss $\nabla_\theta \mathcal{L}$ from a single optimization step. It also incorporates the average score $\bar{u}$ as the features to perform clustering.

Unsupervised Score+Loss Attack (SCORELOSS-UA$_{\text{all}}$) This attack extends SCOREUA$_{\text{all}}$, combining the average loss $\bar{l}$ with the average utility score $\bar{u}$, then aggregating with Φ_{all}.

D ABLATION STUDY

In this section, we provide a detailed analysis of the hyperparameter tuning process for DocMIA in the white-box setting, targeting all the considered models. Given the high computational cost due to the numerous factors involved, we focus on the key parameters that may potentially affect the attack performance. Our intuition behind this tuning process is that: achieving a reliable estimate of the distance Δ requires the optimization process to converge effectively, which in turn correlates with higher attack accuracy. Thus in all of our experiments, to increase the likelihood of convergence, we set the maximum number of optimization steps to $S = 200$. We fix the maximum number of questions per document M to 10.

Learning Rate α We first study the effect of α, which controls the speed of the optimization process in our attacks. This threshold τ is empirically set to be the average loss change observed when performing one optimization step after reaching the correct answer. Only the distance Δ and the number of steps s are used as the features. For FL and FLLoRA attacks, we perform a hyperparameter search over a grid of learning rates, $\alpha \in \{10^{-4}, 0.001, 0.01, 0.1, 0.5, 1.0\}$, and $\alpha \in \{0.1, 0.5, 1.0, 5.0, 10.0, 20.0\}$ for the IG attacks. For FL and FLLoRA, we specifically tune the embedding projection layer, which projects the final hidden states into the vocabulary space, a common design choice across all the target models considered.

As shown in Figure 6(a), setting a high learning rate can cause the optimization process to overshoot, while lower values lead to a more stable but slower convergence. We find that a learning rate of $\alpha = 10^{-3}$ consistently delivers the best attack performance across all models.

The layer to tune L We now investigate the impact of layer selection on the performance of our FL and FLLoRA attacks. All target models in our study follow the transformer encoder-decoder architecture Vaswani (2017), where each component consists of a stack of attention layers, and a shared embedding projection layer maps the hidden states to logit vectors for prediction. Given this common structure, we examine the effect of tuning similar layers across all models, with results for attack accuracy presented in Table 6.

Our findings reveal that *layers closer to the final output exhibit higher privacy leakage* in terms of MI compared to (randomly selected) intermediate layers, likely due to receiving larger gradient updates. Specifically, fine-tuning the final fully connected layer alone leads to strong attack performance while also being more efficient in terms of the number of parameters that need to be optimized. This

Layer	VT5(PFL)	Donut(DocVQA)	Pix2Struct-B(DocVQA)
Embedding Projection Layer	67.0	71.33	68.66
Embedding Layer Norm	65.33	76.0	64.67
Last Decoder Block FC1	**68.33**	**78.0**	68
Last Decoder Block FC2	68.17	77.33	**68.83**
Last Decoder Block Layer Norm	61.83	76.83	67.5
Random Decoder Block FC1	61.33	72.0	67.5
Random Decoder Block FC2	64.0	73.0	65.17

Table 6: **Effect of selected layer to tune** from each target model. Attack performances are reported in terms of Accuracy.

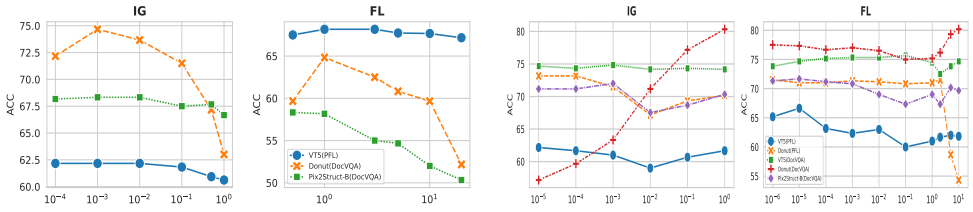

(a) **Learning Rate** α (b) **Threshold** τ

Figure 6: **Ablation Study on Learning Rate** α **and Threshold** τ**.** The best value for each model across all datasets is used as the hyperparameters in our black-box attacks.

suggests that focusing on the last layers can achieve both high privacy leakage and computational efficiency in our MI attacks.

Threshold τ With the optimizer OPT and learning rate α fixed, the threshold τ emerges as the most critical hyperparameter that requires careful tuning for each attack. We experiment with a wide range of τ values, spanning from 10^{-6} to 10.0, and select the optimal value based on attack performance, as demonstrated in Figure 6(b). This optimal τ is then applied consistently in all subsequent experiments. Careful selection of this threshold is crucial, as it directly influences the stability and success of the optimization process.

Model	α_{FL}	α_{IG}	S	L	τ_{FL}	τ_{IG}
VT5		10.0			10^{-6}	1.0
Donut	0.001	0.5	200	last FC layer	1.0	1.0
Pix2Struct-B		0.001			1.0	0.01

Table 7: **Best Hyperaremeters from our tuning process** with consistent performance across both PFL and DocVQA dataset.

We summarize the set of tuned hyperparameters for our approach in Table 7.

E Attack Implementation

E.1 Target Model Training

For all target models, whenever feasible, we utilize the public checkpoint fine-tuned on the considered private dataset from Hugging Face library and adhere to the data processing guidelines, such as document resolution, as recommended by the authors. We deliberately opt for public checkpoints for two reasons: (1) to make it consistent to further research in privacy attacks that use the same trained models, and (2) to minimizing the biases in model training that affect the final results, given the complexity of the original training process and our limited resources. Table 8 summarizes the details of the process from which public checkpoints for the target models considered in this work are obtained. This includes the datasets the models were pre-trained on, before by fine-tuning on target DocVQA datasets, along with the corresponding download URLs for these checkpoints.

Model	Num. Params	Downstream Task	Data		Checkpoint	
			Pretrain	Finetune	Pretrain	Finetune
VT5	250M	DocVQA	C4+IIT-CDIP	PFL DocVQA	https://benchmarks.elsa-ai.eu/?ch=2	
Donut	200M	DocVQA	CDIP 11M + 0.5M synthesized Docs	PFL DocVQA	naver-clova-ix/donut-base†	Ours naver-clova-ix/donut-base-finetuned-docvqa†
Pix2struct-B Pix2struct-L	282M 1.33B	DocVQA	BooksCorpus + C4 Web HTML	DocVQA	google/pix2struct-base† google/pix2struct-large†	google/pix2struct-docvqa-base† google/pix2struct-docvqa-large†

Table 8: **Details of the public checkpoints** used as target models in this work. † denotes checkpoint from Hugging Face.

Model	Optimizer	Learning Rate	Weight Decay	Batch Size	Scheduler	Iteration
VT5	AdamW	2e-4	-	16	-	200k
Donut	Adam	3e-5	0.01	4	Linear Warmup 10%	800k
Pix2Struct-B	AdaFactor	1e-5	-	4	warmup 1000 steps, cosine decay to 0	800k

Table 9: **Details of the training hyperparameter** for each target model in this work.

If public checkpoints are unavailable, we fine-tune the selected model on the respective private dataset, using the pre-trained checkpoint as the initialization, along with the training procedure outlined by the respective authors. To prevent overfitting, we perform early stopping based on validation loss, ensuring that all evaluated models generalize well to previously unseen data. We also use the pre-trained checkpoint to initialize the proxy model $\mathcal{F}_p$ to train it on D_{query}. We provide an overview of the training procedure for each target model, based on the descriptions from the respective papers. These procedures were adapted to fit our computational resources, as outlined in Table 9.

E.2 Target Model Performance on DocVQA

To ensure the utility of the target models for our experiments, we validated that the DocVQA performance of each model checkpoint closely matched the results reported in the respective papers. Table 10 presents the target models' performance across both DocVQA datasets. We observe a clear train-test performance gap, particularly in smaller models, while the gap tends to narrow for more generalized models or with increased dataset size.

E.3 Computation and Runtime

All attack methods are implemented using PyTorch and executed on an NVIDIA GeForce A40 GPU with 45 GB of memory. The maximum runtime for each attack does not exceed *6 hours* per run, depending on the target model's size and the preprocessing steps required for the data. This runtime reflects the efficiency of our approach, especially when compared to methods based on shadow training, which require retraining of large-scale models many times to be effective Carlini et al. (2022). Our results demonstrate that the proposed attacks are both efficient and scalable, making them practical for large-scale models in real-world applications.

F True Positive Rate at low False Positive Rate

In this section, we evaluate our attacks using True Positive Rate (TPR) at fixed False Positive Rate (FPR), following standard practices in recent membership inference attack (MIA) literature. Specifically, we consider TPR at 1% and 3% FPR, as the size of both member and non-member class in D_{test} is 300. For all unsupervised attacks, including baseline methods, the membership score for each document is computed as the Euclidean distance between its feature vector and the centroid of the member cluster obtained via KMEANS clustering.

White-box settings. The evaluation results, presented in Table 11, show that our attacks consistently achieve strong performance, often outperforming or closely matching the best baseline methods across the target models and datasets. Notably, the FL attack demonstrates robustness in the low-FPR regime. For instance, against VT5 trained on PFL, it achieves TPR of 3.67% and 8.67% at

Dataset	Model	Test Set	ACC	ANLS	Train-Test Gap
PFL	VT5	Original	81.4	90.17	-
		MIA	82.74	90.91	11.44
		MIA-rephrased	77.59	85.84	-
	Donut	Original	74.73	88.66	-
		MIA	80.15	91.64	22.2
		MIA-rephrased	70.46	80.96	-
DVQA	VT5	Original	60.1	69.33	-
		MIA	75.54	81.69	36.22
		MIA-rephrased	73.57	79.89	-
	Donut	Original	59.26	66.91	-
		MIA	78.55	83.42	39.78
		MIA-rephrased	72.57	77.12	-
	Pix2Struct-B	Original	57.11	68.13	-
		MIA	64.42	79.95	25.8
		MIA-rephrased	63.81	74.06	-
	Pix2Struct-L	Original	64.53	74.12	-
		MIA	73.91	82.71	22.11
		MIA-rephrased	69.93	79.15	-

Table 10: **DocVQA Performance of the target models on PFL and DocVQA dataset.** Train-Test Gap is computed as the different of DocVQA Accuracy between *member/non-member* documents. MIA denotes the attack evaluation set, which is a subset randomly sampled from the original train/test set, MIA-rephrased is its variants with rephrased questions by LLM.

	DVQA						**PFL**			
	VT5		Donut		Pix2Struct-B		VT5		Donut	
	1%	3%	1%	3%	1%	3%	1%	3%	1%	3%
LOSS-TA	**7.67**	**14.00**	0.67	7.67	2.33	5.33	0.67	3.00	1.67	**14.67**
GRADIENT-UA	2.33	9.33	3.67	6.00	1.00	5.00	0.33	3.00	1.00	8.33
SCORELOSS-UA$_{\text{all}}$	1.33	4.67	2.67	8.67	2.00	6.67	0.33	4.00	0.67	6.33
Min-K%	2.67	10.67	0.33	1.33~~(1.00)~~	0.33	5.33	1.67	5.67	0.00	0.00
Min-K%++	1.00~~(2.67)~~	7.00~~(10.00)~~	**4.33**~~(0.33)~~	9.33	0.67~~(0.33)~~	10.33	1.00~~(1.67)~~	8.00	0.33~~(0.00)~~	2.00~~(1.67)~~
FL	2.33	5.67	3.33	**10.67**	**6.00**	**11.00**	**3.67**	**8.67**	0.33	7.00
FLLoRA	3.33	11.33	2.67	5.33	3.67	6.33	1.33	3.33	0.33	10.00
IG	0.67	5.67	1.33	8.00	3.00	10.33	1.00	2.33	**5.67**	11.00

Table 11: **White-box: TPR at fixed FPR**. Comparison across all white-box methods, with the best-performing method for each metric highlighted in **bold**. 1% and 3% indicate TPR@1%FPR and TPR@3%FPR respectively.

1% and 3% FPR, respectively, despite this model exhibits minimal overfitting. On DocVQA, FL achieves TPRs of 6.00% and 11.00% at the same FPR thresholds against Pix2Struct-B.

An interesting observation is the high performance of the LOSS-TA method for VT5 on DocVQA and Donut on PFL. This performance can be attributed to the clear separation in the loss distribution between member and non-member samples (Figure 7), which indicates overfitting behavior in these cases.

We also compare our attacks to two recent baselines, Min-K% Shi et al. (2023) and Min-K%++ Zhang et al. (2024), originally designed for detecting pre-trained data in LLMs. Using the official code, we adapt these methods for the DocMIA setting as followed: (1) we aggregate Min-K% scores across all questions for each document using the AVG function and (2) since predicted answers in DocVQA models are much shorter than those generated by LLMs, we evaluated $K \in [0.6, 0.7, 0.8, 0.9, 1.0]$, which correspond to corresponds to 60% to 100% the length of the answer and reported the best result. Our methods outperform both Min-K% and Min-K%++ in MIA performance across all target models, highlighting the effectiveness of our attack design, particularly in the context of DocMIAs.

Black-box settings. The results for black-box evaluation are presented in Table 12. We observe that using VT5 as a proxy model for our attacks generally leads to strong performance, for instance against Donut and Pix2Struct-B on DocVQA. This can be attributed to the large Train-Test utility gap observed in the target models (Table 10), which enables the proxy model to closely mimic the black-box model's predictions and enhance attack effectiveness.

Proxy	Target	DVQA								PFL			
		VT5		Donut		Pix2Struct-B		Pix2Struct-L		VT5		Donut	
		1%	3%	1%	3%	1%	3%	1%	3%	1%	3%	1%	3%
	SCORE-TA	4.00	9.33	5.00	11.00	3.33	9.00	3.33	**9.00**	1.00	5.00	0.67	2.67
	SCORE-UA	3.67	7.67	4.33	15.67	4.33	6.67	4.33	6.67	0.67	3.33	0.33	3.33
	SCORE-UA$_{\text{all}}$	4.00	9.33	5.00	11.00	3.33	9.00	3.33	9.00	1.00	5.00	0.67	2.67
VT5	FL	0.67	12.33	**11.67**	**23.00**	2.00	**16.67**	2.00	5.33	0.67	2.00	**5.00**	**8.00**
	FLLoRA	**4.67**	**11.33**	11.67	23.00	2.33	9.33	1.00	4.67	2.00	3.33	0.00	2.00
	IG	1.00	8.33	2.00	7.00	**4.67**	7.67	2.33	7.00	0.33	3.67	1.33	6.67
Donut	FL	0.33	6.33	0.33	4.00	1.33	4.67	3.00	7.33	0.33	1.33	1.33	4.00
	FLLoRA	1.00	6.33	0.33	4.00	2.33	6.33	3.00	8.00	0.00	5.33	2.00	5.33
	IG	1.67	5.00	0.67	11.00	3.67	9.33	**4.67**	6.33	**2.67**	**6.33**	1.67	4.33

Table 12: **Black-box: TPR at fixed FPR**. Comparison across all black-box methods, with the best-performing method for each metric highlighted in **bold**. 1% and 3% indicate TPR@1%FPR and TPR@3%FPR respectively.

	White-box	FL		FLLoRA		IG	
		ACC	F1	ACC	F1	ACC	F1
PFL	VT5	**66.63$_{0.07}$(+5.96)**	**72.40$_{0.1}$(+11.73)**	65.17$_{0.0}$(+4.50)	70.52$_{0.0}$(+9.85)	61.83$_{0.0}$(+1.16)	69.18$_{0.0}$(+8.51)
	Donut	72.67$_{0.0}$(+1.5)	77.96$_{0.0}$(+6.63)	72.83$_{0.0}$(+1.66)	77.94$_{0.0}$(+6.61)	**75.17$_{0.0}$(+4)**	**79.39$_{0.0}$(+8.06)**
DVQA	VT5	75.67$_{0.0}$(+0.5)	76.60$_{0.0}$(+1.47)	75.57$_{0.08}$(+0.4)	77.31$_{0.13}$(+2.18)	74.83$_{0.0}$(−0.34)	76.88$_{0.0}$(+1.75)
	Donut	80.33$_{0.0}$(−0.17)	82.18$_{0.0}$(+1.08)	80.0$_{0.0}$(−0.5)	81.93$_{0.0}$(+0.83)	80.33$_{0.0}$(−0.17)	82.34$_{0.0}$(+1.24)
	Pix2Struct-B	71.67$_{0.0}$(+2.54)	72.22$_{0.0}$(+4.55)	70.50$_{0.0}$(+1.37)	71.95$_{0.0}$(+4.28)	**72.00$_{0.0}$(+2.87)**	**72.82$_{0.0}$(+5.15)**

Table 13: **White-Box: Main Results of DocMIA.** Values in parentheses indicate the improvement (positive/negative) of our proposed attacks compared to the SCORELOSS-UA$_{\text{all}}$. Compared to all baselines, the methods with the best *average* performance across the two metrics are highlighted in **bold**. Results are reported over five random seeds.

G MORE ON ANALYSIS

In this section, we provide a deeper analysis of the effectiveness of our proposed white-box and black-box attacks, highlighting their performance relative to the baseline approaches.

G.1 IMPACT OF SELECTED FEATURES

As outlined in the main paper, we fix the set of selected features across all experiments. These features include the DocVQA score u, the optimization-based distance Δ, and the number of optimization steps s, aggregated using the set of aggregation functions $\Phi_{\text{all}} = \{\text{AVG}; \text{MIN}; \text{MAX}; \text{MED}\}$. We first evaluate the impact of individual features and their combinations on attack performance in the white-box DocMIA setting, using AVG as the aggregation function Φ. The analysis employs the best hyperparameters identified during the tuning process described in Section D. For the DocVQA score u, we use the Normalized Levenshtein Similarity (NLS) metric, which measures the similarity between the predicted answer $\hat{a}$ and the ground-truth answer a:

$$\text{NLS} = \begin{cases} 1 - \text{NL}(\hat{a}, a) & \text{if } \text{NL}(\hat{a}, a) < 0.5, \\ 0 & \text{if } \text{NL} \geq 0.5 \end{cases} \tag{3}$$

where $\text{NL}(\cdot, \cdot)$ denotes the normalized Levenshtein distance.

Table 14 and Table 16 summarize the attack performance when individual features or their combinations are used. Additionally, Table 15 *(Top)* compares the attack performance of our optimization-based features with the loss value ℓ and the gradient norm of the loss with respect to the model parameters θ. Here, the loss value ℓ is computed uniformly across all target models over K generation steps, given a (document, question, answer) example (x, q, a) as:

$$\ell = -\sum_{k=1}^{K} \log p_\theta(a_k | a_{<k}, x, q) \tag{4}$$

When used individually, our proposed optimization-based features outperform the DocVQA score and the loss in most cases. Our attack methods are particularly effective against target models like

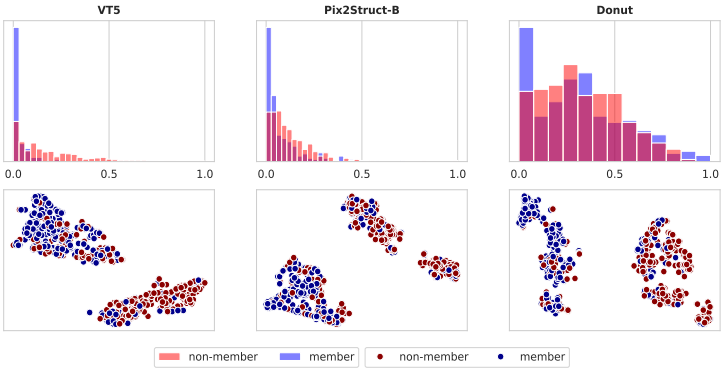

Figure 7: **Membership Features against three different target models on DocVQA Dataset.** *Top*: The distribution of average ***loss*** over all questions from all target documents on each target model. *Bottom*: T-SNE visualization of the features used in our proposed attacks.

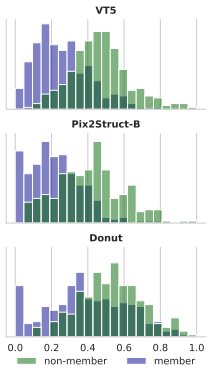

Figure 8: **Distribution of Average *Distance*:** Comparing the ability of the *distance* feature to differentiate between member and non-member documents across three models.

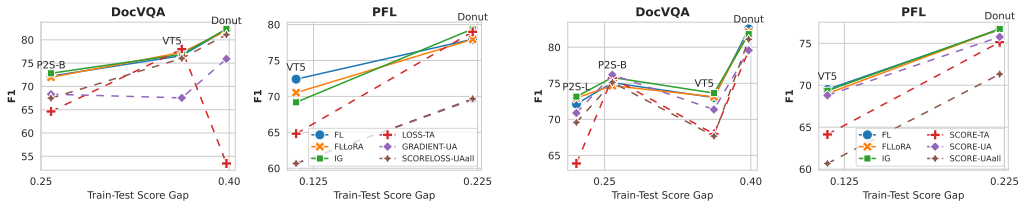

(a) **White-box** (b) **Black-box**

Figure 9: **MI performance versus the Train-Test gap.** The target models exhibit varying Train-Test gaps, measured by the difference in DocVQA scores between member and non-member documents. Our proposed attacks remain effective even when the gap is small, with performance steadily improving as the gap increases across most target models and datasets. In contrast, baseline methods show more variable performance under these conditions.

VT5 and Donut trained on PFL-DocVQA, which exhibit lower overfitting and small Train-Test gaps (as shown in Table10). These results highlight that our attacks provide more discriminative features than the commonly used MIA features.

When combined, our selected features achieve the best or near-best performance across all cases. Furthermore, extending aggregation functions from AVG to Φ_{all} adds notable improvements in attack effectiveness, as shown in Table 15 *(Bottom)*. These results demonstrate that our proposed feature set is robust across different target models, making it a reliable choice for DocMIA.

G.2 Impact of the Training Questions Knowledge

So far, our document MI attacks against DocVQA models have assumed complete knowledge of the original training questions. We now relax this assumption and investigate how the lack of access to the exact training questions affects attack performance. In practice, an adversary may not have access to the exact training questions but can approximate them. For example, documents like invoices often follow standard layouts, and biases in human annotation may lead to predictable patterns in the types of questions asked during the creation of DocVQA datasets Tito et al. (2024); Mathew et al. (2021). It is important to note that the original training questions tend to be simple, natural questions designed to extract specific information from the document. Moreover, the type of question is inherently linked to the type of document on which the DocVQA model is trained. For instance, if the target model is trained on invoices, the natural type of question would focus on extracting essential details from the invoice, such as the "total amount", framed in a clear and

VT5				Donut			
AVG(NLS)	AVG(Δ)	AVG(s)	F1	AVG(NLS)	AVG(Δ)	AVG(s)	F1
✓			68.88	✓			67.58
	✓		71.5		✓		71.36
		✓	70.92			✓	73.16
✓	✓		71.09	✓	✓		72.87
✓		✓	71.11	✓		✓	73.67
	✓	✓	71.22		✓	✓	73.86
✓	✓	✓	**71.53**	✓	✓	✓	**73.89**

Table 14: **Impact of Selected Features on PFL-DocVQA Models.**

	PFL		DVQA		
	VT5	Donut	VT5	Donut	Pix2Struct-B
AVG(ℓ)	67.53	67.80	73.43	56.79	69.97
AVG($\|\|\nabla_\theta \mathcal{L}\|\|_2$)	70.53	71.51	71.91	71.53	66.14
AVG(Δ)	71.45	71.36	72.86	57.34	70.57
AVG(s)	70.92	73.16	74.34	60.32	69.00

	PFL		DVQA		
	VT5	Donut	VT5	Donut	Pix2Struct-B
Φ = AVG	71.53	73.89	74.96	72.94	73.22
$\Phi = \Phi_{\text{all}}$	72.4(+0.87)	77.96(+4.07)	76.6(+1.67)	82.18(+9.24)	72.22(-1.0)

Table 15: **Comparisons in Attack Performance in terms of F1 Score**: *(Top)* between our Optimization-based Features with the loss value ℓ and the gradient norm $||\nabla_\theta \mathcal{L}||_2$. *(Bottom)* between AVG and Φ_{all} as the aggregation functions.

VT5				Donut				Pix2Struct-B			
AVG(NLS)	AVG(Δ)	AVG(s)	F1	AVG(NLS)	AVG(Δ)	AVG(s)	F1	AVG(NLS)	AVG(Δ)	AVG(s)	F1
✓			72.73	✓			**76.88**	✓			72.60
	✓		72.86		✓		57.34		✓		70.57
		✓	74.34			✓	60.32			✓	69.00
✓	✓		**75.81**	✓	✓		65.94	✓	✓		73.20
✓		✓	75.04	✓		✓	72.17	✓		✓	72.87
	✓	✓	74.19		✓	✓	60.29		✓	✓	70.17
✓	✓	✓	74.96	✓	✓	✓	72.94	✓	✓	✓	**73.22**

Table 16: **Impact of Selected Features on DocVQA Target Models**. Only AVG is used as the aggregation function Φ. Attack performances are obtained with our FL method using the best hyperparameters.

straightforward manner e.g., "What is the total?". This makes it possible for an adversary to generate approximate versions of the training questions, simulating a more realistic attack setting.

	Model	SCORE-TA		SCORE-UA$_{\text{all}}$		LOSS-TA		SCORELOSS-UA$_{\text{all}}$		OURS (FL)	
		ACC	F1	ACC	F1	ACC	F1	ACC	F1	ACC	F1
PFL	VT5	60.67	64.13	$55.83_{0.0}$	$46.89_{0.0}$	54.50	59.19	$55.83_{0.0}$	$46.89_{0.0}$	**$64.00_{0.0}$**	**$69.14_{0.0}$**
	Donut	69.17	69.72	$59.33_{0.0}$	$51.59_{0.0}$	68.50	66.67	$59.17_{0.0}$	$51.49_{0.0}$	**$71.13_{0.08}$**	**$72.07_{0.0}$**
DVQA	VT5	73.67	75.01	$74.83_{0.0}$	$74.36_{0.0}$	71.67	74.06	$75.17_{0.0}$	$74.96_{0.0}$	**$74.83_{0.0}$**	**$75.68_{0.0}$**
	Donut	**69.17**	**71.23**	$65.17_{0.0}$	$62.21_{0.0}$	52.33	53.57	$65.17_{0.0}$	$62.21_{0.0}$	$67.67_{0.0}$	$68.51_{0.0}$

Table 17: **Results with Rephrased Questions.** Gray color indicate attacks conducted in the black-box setting. All results are reported based on five random seeds. The methods with the best *average* performance across the two metrics are highlighted in **bold**.

To explore this scenario, we conduct experiments where we paraphrase the original training questions using Mistral Jiang et al. (2023), and use these rephrased questions as inputs for the MI attacks. As illustrated in Table 17, the performance of all MI attacks declines when rephrased questions are used, mirroring the drop in DocVQA model performance (Table 10), which is expected due to the increased uncertainty introduced by question rephrasing.

Among the baselines, the SCORE-TA attack proves particularly to be robust, especially against models trained on DocVQA, which show a higher degree of overfitting. In contrast, attacks incorporating loss-based signals introduce additional noise due to uncertainty, leading to a noticeable drop in performance.

Despite the rephrasing, our attacks remain effective, maintaining performance levels comparable to those observed with the original questions, especially against the two PFL models, which demonstrate a lower degree of overfitting.

We also evaluate our proposed attacks against other methods in this setting, focusing on TPR at 1% and 3% FPR, with the results summarized in Table 19 and 20.

		FL				IG			
PFL	Model	$m = 1(1)$	$m = 2(1)$	$m = 3(85)$	ALL(300)	$m = 1(1)$	$m = 2(1)$	$m = 3(85)$	ALL(300)
	VT5	0	0	83.53	87.67	100	100	85.88	86.33
	Donut	100	100	100	97.67	100	100	97.65	97
DVQA	Model	$m = 1(51)$	$m = 2(60)$	$m = 3(52)$	ALL(300)	$m = 1(51)$	$m = 2(60)$	$m = 3(52)$	ALL(300)
	VT5	86.27	71.67	84.62	77.00	90.2	85	86.54	80.67
	Donut	88.24	73.33	76.92	77.33	56.86	68.33	55.77	61.33
	Pix2Struct-B	90.2	93.33	90.38	87	88.24	88.33	76.92	73

Table 18: **Membership Prediction Accuracy on *Member* Documents with minimal repetition.** m denotes the subset of testing documents with m *training* questions, with subset sizes shown in parentheses. Compared to the performance measured on the entire member set (denoted as ALL), our attacks are still robust against documents with the low risk of memorization.

G.3 The Resulting Proxy Model

The purpose of training the Proxy Model on D_{query}, with labels generated by the black-box model, is to mimic the prediction patterns of the black-box model. The expectation is that the proxy model can capture internal decision-making patterns by following the black-box's prediction strategies. Instead of optimizing for ground-truth labels, we train the proxy to maximize the likelihood of the generated labels. The training process concludes when the proxy achieves near-zero training loss, at which point the final checkpoint is used for the attack. As illustrated in Figure 10(a), the

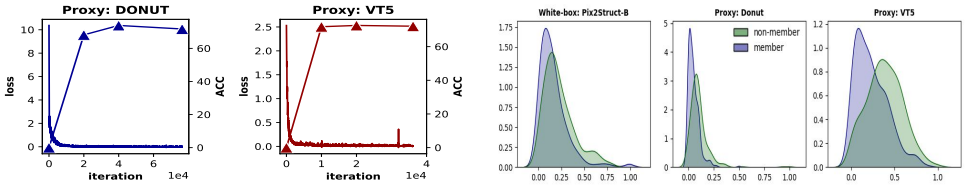

(a) **Training curve** (b) **Distribution over distance**

Figure 10: **The resulting Proxy Model** against Pix2Struct-B in the black-box setting. (*a*) The attack accuracy improves quickly once the loss reaches near zero. (*b*) The optimization distance values between member and non-member documents exhibit a separation similar to that seen in the white-box setting.

attack performance quickly improves as training progresses. The model overfits quickly, with attack performance reaching its peak early—after just a quarter of the training process—demonstrating the efficiency of our approach. This suggests that *once the proxy model converges, it has effectively captured informative membership signals from the black-box model*, making it ready for the attack. Moreover, we compare the distribution of optimization distances between the proxy model and the same model in the white-box setting, as shown in Figure 10(b). The results show a similar degree of separation between the two clusters in both cases, indicating the proxy model's effectiveness in approximating the black-box model's behavior to a certain extent.

G.4 Attack Performance against Minimal-Training Documents

DocVQA models typically process each question-answer pair independently, resulting in multiple exposures of each document during training. This increases the likelihood of being memorized by the model, making such documents more vulnerable to MIAs. Intuitively, documents associated with fewer training questions should be less exposed and therefore be less vulnerable.

To evaluate this, we measure the accuracy of membership predictions from our attacks on a subset of *member* documents in D_{test} associated with only a few training questions. These documents represent a minimal memorization risk, posing a more challenging evaluation scenario. Results in Table 18 show that our attacks remain effective on these subsets, achieving high accuracy even for documents $m = 1$ training question. This demonstrates the robustness of our attacks under conditions of minimal repetition.

	DVQA				PFL			
	VT5		Donut		VT5		Donut	
	1%	3%	1%	3%	1%	3%	1%	3%
Min-K%	3.00	4.33	0.33	1.00	**6.33**	**20.33**	2.00	2.33
Min-K%++	3.00	4.67	0.00	2.67	6.33	10.00	0.00	7.00
FL	0.67	5.00	**3.33**	**8.00**	3.67	17.33	3.00	4.67
FLLoRA	**5.00**	**9.33**	0.67	3.67	5.00	9.33	**4.33**	**10.00**
IG	5.33	8.00	1.00	5.00	5.33	8.00	1.67	10.00

Table 19: **White-box Results: TPR at 1% and 3% FPR with Rephrased Questions**. Comparison to *white-box* methods: Min-K% and Min-K%++ methods, with the best method in **bold**.

	PFL		DVQA			
	VT5		Donut		Pix2Struct-B	
	1%	3%	1%	3%	1%	3%
SCORE-TA	0.33	2.67	**3.33**	9.67	3	8.67
SCORE-UA$_{\text{all}}$	0.33	2.67	2.33	9.33	**4.67**	8.67
FL	0.33	1.33	0.33	4.00	1.33	4.67
FLLoRA	1.00	5.33	1.67	5.00	2.33	6.33
IG	**2.67**	**6.33**	1.67	**11.00**	3.67	**9.33**

Table 20: **Black-box Results: TPR at 1% and 3% FPR with Rephrased Questions**. Donut is used as The Proxy Model.

H DEFENSES

To mitigate the privacy vulnerabilities associated with membership inference attacks in Document Visual Question Answering (DocVQA) systems, we can employ Differential Privacy (DP) techniques (Dwork et al., 2014), specifically through the use of differentially private stochastic gradient descent (DP-SGD) introduce by Abadi et al. (2016). DP is a robust framework that ensures an individual's data contribution cannot be inferred, even when an adversary has access to the model's outputs. DP-SGD achieves this by adding calibrated noise to the model's gradients during training, thus providing strong theoretical privacy guarantees. However, this approach is not without its drawbacks; the necessity of noise injection can adversely affect the utility of the trained model, leading to reduced performance in answering queries accurately. Alternatively, we can consider ad-hoc solutions such as limiting the number of queries to one question per document in black-box setting, which would inherently reduce the model's usability and flexibility in practical applications. While these measures can enhance privacy, they also necessitate careful consideration of the balance between privacy protection and the functionality of DocVQA systems.

To evaluate the robustness of our proposed membership inference attacks against Differential Privacy (DP), we implemented the well-known DP-SGD algorithm. We considered five privacy budget $\varepsilon \in \{8, 32\}$, with corresponding noise multiplier $\sigma \in \{0.5767822266, 0.3824234009\}$, respectively. The composition of the privacy budget over multiple iterations was calculated using Rényi Differential Privacy (RDP). We then converted the RDP guarantees into the standard (ε, δ)-DP notion following the conversion theorem from Balle et al. (2020).

We trained the Donut model on the DocVQA dataset with DP-SGD to provide theoretical privacy guarantees for individual training documents. Due to resource constraints, we resized document resolution to a smaller size (1280, 960) compared to (2560, 1920) in the public checkpoint provided by the original authors, which slightly reduced the model's DocVQA performance. For additional details on the effects of document resolution, we refer readers to the original model's paperKim et al. (2022). The model was trained using the Adam optimizer with a learning rate of $1e-4$, for 10 epochs, and with a batch size of 16. DocVQA performance was evaluated using the Average Normalized Levenshtein Similarity (ANLS) metric.

Table 21 summarizes the results. As expected, introducing DP into model training significantly reduces the attack performance, for example from 73.81% F1 score with non-DP model to 55.09% at $\varepsilon = 8$, but this comes at the cost of substantial utility degradation, with the DP model achieving less than half of the performance of the non-DP model, 21.81 of ANLS at $\varepsilon = 8$ compared to 50.12 of ANLS from non-DP checkpoint. For higher privacy budgets ($\varepsilon = 32$), our attacks demonstrate improved effectiveness, achieving notable gains, +3.75 in F1 and +2 in TPR3%FPR scores compared to $\varepsilon = 8$, as the model becomes less privacy-constrained.

	$\varepsilon = 8$			$\varepsilon = 32$			$\varepsilon = \infty$		
	ANLS	F1	TPR@3%FPR	ANLS	F1	TPR@3%FPR	ANLS	F1	TPR@3%FPR
FL		55.09	2.33		58.84	4.33		73.81	7.33
FLLoRA	19.16	54.94	2.00	21.81	58.94	3.67	50.12	73.81	7.33
IG		56.29	1.67		59.35	5.00		73.52	8.67

Table 21: **DocMIA Results for Donut trained with DP-SGD on DocVQA dataset**. We report the attack performance of our FL method in terms of F1 score and TPR3%FPR.